Electronic Supplementary Material (ESI) for ChemComm.

The template effect of a SiF_6^{2-} guest drives the formation of a heteroleptic Fe(II) coordination helicate

Nuria Capó,[a] Leoní A. Barrios,*,[a] Joan Cardona,[a] Jordi Ribas-Ariño,[b] Simon J. Teat,[c] Olivier Roubeau[d] and Guillem Aromí*,[a]

Supporting Information

Synthesis

3,3'-diacetylbiphenyl was prepared according to a procedure described in the literature.[1] $(Bu_4N)_2SiF_6$ was prepared by mixing 2 equivalents of Bu_4NOH (55% in water solution) with 1 equivalent of H_2SiF_6 (20% solution in water). The resulting salt was collected by filtration, washed with diethyl ether and dried under vacuum.

3,3'-bis[1-(4-picolin-2-yl)propane-1,3-dione)-1,1'-biphenyl (L3')

Under N_2 atmosphere, a suspension of a 60% NaH oil dispersion (0.5 g, 12.5 mmol) was washed with hexane and the supernatant was removed with a Pasteur pipette in order to separate the mineral oil. Dry THF (50 mL) was then added, followed by the addition of 3,3'-diacetylbiphenyl (0,6 g, 2.5 mmol) dissolved in dry THF (50 mL). The resulting grey mixture, was stirred for 15 min. and then 4-methylpyridine-2-carboxylate (0.67 ml, 5 mmol) was added dropwise to it, turning into a yellowish mixture that was left to reflux overnight. Some drops of methanol were then added to quench the unreacted NaH and the red-orange solution was cooled and evaporated under reduced pressure to dryness. The reddish solid obtained was suspended in water and stirred for 20 min. With further stirring, the mixture was acidified using HCl (37%) to adjust the pH into the range 2-3, producing a change of color to yellow and the precipitation of a yellowish solid. After 15 minutes under stirring, the yellow-green solid was recovered by filtration, washed with water several times and dried under vacuum.

Green solid. Yield(%): 38. ^1H NMR ($CDCl_3$, 400MHz): 16.47 (broad s, 2H), 8.50 (d, 2H), 8.25 (s, 2H), 8.02 (d, 2H), 7.95 (s, 2H), 7.77 (d, 2H), 7.53 (m, 4H), 2.35 (s, 6H).

3,3'-bis(3-(4-picolin-2-yl)-1H-pyrazol-5-yl)-1,1'-biphenyl (L3).

The bis-β-diketone L3' (1.0 g, 2.1mmol) was suspended in methanol (100 mL). Hydrazine monohydrate (21 mmol) was added dropwise and the resulting brown suspension and the mixture was left to reflux overnight. The resulting yellow suspension was cooled to room temperature and evaporated to dryness under reduced pressure, giving a sticky beige solid, which was suspended in water and stirred for 30 minutes. The suspension was filtrated to separate the resulting beige solid, which was washed several times with water and with small portions of chloroform before being dried under vacuum.

---

[1] 1. H.-F. Li, P.-F. Yan, P. Chen, Y. Wang, H. Xu and G.-M. Li, *Dalton Trans.*, 2012, **41**, 900–7.

Light beige solid. Yield(%): 69. IR: 3223, 1607, 1576, 1095, 1057, 963, 813, 778. ^{1}H NMR (Acetone, 400MHz): δ 8.48 (d, 2H), 8.32 (s, 2H), 7.96 (d, 2H), 7.83 (s, 2H), 7.75 (d, 2H), 7.58 (t, 2H), 7.44 (s, 2H), 7.16 (t, 2H), 2.42 (s, 6H). m/z ESI+ 469.213[L3+H]$^+$, 937.421 [2(L3)+H]$^+$, 235.109 [L3+2H]$^+$.

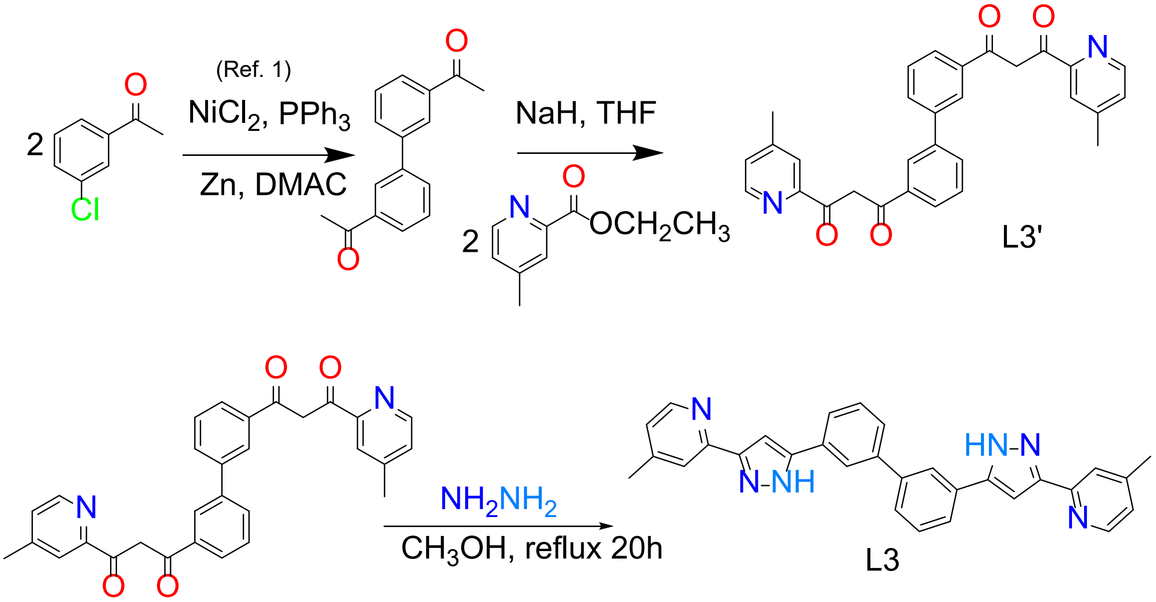

Figure S1. Scheme of the synthetic procedure employed for the preparation of L3.

SiF_6@[Fe_2(L1)(L2)$_2$](PF_6)$_2$ (1). Inside of a glove box with N_2 atmosphere, a solution of L1 (8.3 mg, 0.023 mmol) and L2 (20 mg, 0.046 mmol) in methanol (10 mL) was added dropwise onto a stirred solution of $Fe(BF_4)_2$ (14.5 mg, 0.063 mmol) and ascorbic acid (2 mg) in methanol (5 mL). The stirring was maintained for 45 minutes, leading to a colour change from yellow to orange and to cloudiness. The cloudy solution was filtered with a nylon membrane with pores of 0.22 μm of diameter. The filtrate was combined with a solution containing an excess of Bu_4NPF_6 (33.5 mg, 0.87 mmol) in MeCN (5 mL), the mixture was then stirred for 10 minutes and filtered. The filtrated was transferred to a "pyrex 15" tube. Upon slow diffusion of diethyl ether, yellow needles of **1** formed after 15 days. Yield 21%. *Anal. Calc.* (Found) for **1**·3.1CH_3OH: C, 51.65 (51.87); H, 3.87 (3.62); N, 13.04 (12.80).

SiF_6@[Fe_2(L1)(L2)$_2$](BF_4)$_2$ (1a). A solution of L1 (8.3 mg, 0.023 mmol) and L2 (20 mg, 0.046 mmol) in methanol (10 mL) was added dropwise onto a stirred solution of $Fe(BF_4)_2$ (14.5 mg, 0.063 mmol) and ascorbic acid (2 mg) in methanol (5 mL). The stirring was maintained for 45 minutes, leading to a colour change from yellow to orange and to cloudiness. The cloudy solution was filtered with a nylon membrane with pores of 0.22 μm of diameter and transferred to a polypropylene tube. This solution was put into contact with a solution of $(Bu_4N)_2SiF_6$ (28.8 mg, 0.046 mmol) in DMF (4 mL) for slow diffusion. Yellow blade shaped crystals of **1a** formed after 15 days. Yield 39.5%. *Anal. Calc.* (Found) for **1a**·$1.6CH_3OH·5.5H_2O$: C, 53.66 (53.58); H, 4.17 (4.08); N, 13.72 (13.63).

SiF_6@[Fe_2(L1)(L3)$_2$](PF_6)$_2$ (2). Inside of a glove box with N_2 atmosphere, a stirred solution of L1 (7.8 mg, 0.021 mmol) and L3 (20 mg, 0.043 mmol) in methanol (10 mL) was added dropwise onto a stirred solution of $Fe(BF_4)_2·6H_2O$ (14.5 mg, 0.063 mmol) and ascorbic acid (2 mg) in methanol (5 mL). The stirring was maintained for 45 minutes, leading to a colour change from yellow to orange and to cloudiness. The cloudy solution was filtered with a nylon membrane with pores of 0.22 μm of diameter. The filtrate was combined with a solution containing an excess of Bu_4NPF_6 (33.5 mg, 0.87 mmol) in MeCN (5 mL), the mixture was then stirred for 10 minutes and filtered. The filtrated was transferred to a "pyrex 15" tube. Upon slow diffusion of toluene, yellow needles of **2** formed after 15 days. Yield 12.35%. *Anal. Calc.* (Found) for **2**·$3.1CH_3OH$: C, 52.56 (52.24); H, 3.96 (3.53); N, 12.96 (12.54).

SiF_6@[Fe_2(L1)(L3)$_2$](BF_4)$_2$ (2a). A solution of L1 (7.8 mg, 0.021 mmol) and L3 (20 mg, 0.043 mmol) in methanol (10 mL) was added dropwise onto a stirred solution of $Fe(BF_4)_2$ (14.5 mg, 0.063 mmol) and ascorbic acid (2 mg) in methanol (5 mL). The stirring was maintained for 45 minutes, leading to a colour change from yellow to orange and to cloudiness. The cloudy solution was filtered with a nylon membrane with pores of 0.22 μm of diameter and transferred to a polypropylene tube. This solution was put into contact with a solution of $(Bu_4N)_2SiF_6$ (27.0 mg, 0.043 mmol) in DMF (2 mL) for slow diffusion. Yellow blade shaped crystals of **2a** formed after 10 days. Yield 40.32%. *Anal. Calc.* (Found) for **2a**·$0.1CH_3OH·5.58H_2O$: C, 53.66 (53.58); H, 4.17 (4.08); N, 13.72 (13.63).

ClO_4@[Fe_2(L2)$_3$](ClO_4)$_3$ (3).

Method A: A suspension of L2 (30 mg, 0.068 mmol) in methanol (10 mL) was added dropwise to a methanolic solution (5 mL) of $Fe(ClO_4)_2$ (12 mg, 0.047 mmol) and 2.0 mg of ascorbic acid. An orange slightly cloudy solution formed, which was stirred for 45 minutes and then filtered. The resulting solution was treated with NBu_4ClO_4 (93 mg, 0.27 mmol) in 3 mL of MeCN and stirred for 10 minutes. The orange solution was put inside a closed vessel at room temperature and left into contact with ether vapors that slowly diffused into it, yielding orange crystals after few days (8.0 mg, 18% yield).

Method B: A suspension of L2 (25 mg, 0.057 mmol) in methanol (10 mL) was added dropwise to a methanolic solution (5 mL) of $Fe(CF_3SO_3)_2·6H_2O$ (17.4 mg, 0.038mmol). A red solution formed, which was stirred for 45 minutes and then filtered. The resulting filtrate was treated with a methanolic solution (5ml) of excess of NBu_4ClO_4 (130 mg, 0.38 mmol) and stirred for 10 minutes which yielded a heavy precipitate. The solid was collected by filtration and then dissolved in acetonitrile. The red solution was put inside a closed vessel at 5 ºC and left into contact with ether vapors that slowly diffused into it, yielding red crystals after few days. The yield was 10.2 mg (21.6 %). *Anal. Calc.* (Found) for **3**·6H_2O: C, 52.29 (51.98); H, 3.89 (3.61); N, 13.86 (13.49).

ClO_4@[Fe_2(L3)$_3$](ClO_4)$_3$ (4). A suspension of L3 (32 mg, 0.068 mmol) in methanol (10 mL) was added dropwise to a methanolic solution (5 mL) of $Fe(ClO_4)_2$ (12 mg, 0.047 mmol) and 1.5 mg of ascorbic acid. An orange solution formed, which was stirred for 45 minutes and then filtered. The resulting solution was treated with a methanolic solution (3ml) of NBu_4ClO_4 (93 mg, 0.27 mmol) and stirred for 10 minutes. The red solution was put inside a closed vessel at 5 ºC and left into contact with ether vapors that slowly diffused into it, yielding red crystals after few days (8.0 mg, 18% yield). The yield was 10.2 mg (21.6 %). *Anal. Calc.* (Found) for **4**·7.2H_2O: C, 52.86 (52.50); H, 4.26 (3.81); N, 12.33 (12.11).

Single-crystal X-ray diffraction

Data for compound **1** were collected at 100 K at Beamline 12.2.1 of the Advanced Light Source (Berkeley, USA), on a Bruker D8 diffractometer equipped with a PHOTON II detector and using silicon (111) monochromated synchrotron radiation (λ = 0.7288 Å). Data for compounds **1a**, **2**, **2a** and **4** were acquired at 100 K on the BL13-XALOC beamline[2] of the ALBA synchrotron (λ = 0.72932 Å). Data for **3** were obtained at 100 K with a Bruker APEX II QUAZAR diffractometer equipped with a microfocus multilayer monochromator with Mo Kα (λ = 0.71073 Å). Data reduction and absorption corrections for **1** and **3** were performed with respectively SAINT and SADABS.[3] Data reduction for compounds **1a**, **2a** and **4** were done with autoproc package[4] and XDS.[5] Data reduction and absorption corrections for compound **2** were done with autoproc package,[4] XIA2[6] and AIMLESS.[7] All structures were solved by intrinsic phasing with SHELXT[8] and refined by full-matrix least-squares on F^2 with SHELXL.[9] The measured crystal for **4** happened to be twinned, which was detected through verification with PLATON. PLATON/TwinRotMat[10] was used to find the twin law and to generate the HKLF 5 file

---

[2] J. Juanhuix, F. Gil-Ortiz, G. Cuní, C. Colldelram, J. Nicolás, J. Lidón, E. Boter, C. Ruget, S. Ferrer and J. Benach, *J. Synchrotron Radiat.*, 2014, **21** , 679-689.

[3] a) G. M. Sheldrick, *SAINT and SADABS*, 2012, Bruker AXS Inc., Madison, Wisconsin, USA; b) L. Krause, R. Herbst-Irmer, G. M. Sheldrick, D. Stalke, *J. Appl. Cryst.*, 2015, **48**, 3-10.

[4] C. Vonrhein, C. Flensburg, P. Keller, A. Sharff, O. Smart, W. Paciorek, T. Womack, and G. Bricogne, *Acta Cryst. D,* 2011, **67**, 293-302.

[5] W. Kabsch, *Acta Cryst. D* 2010, **66**, 125-132.

[6] a) G. Winter, J. Appl. Cryst., 2010, 43, 186-190; b) G. Winter, D. G. Waterman, J. M. Parkhurst, A. S. Brewster, R. J. Gildea, M. Gerstel, L. Fuentes-Montero, M. Vollmar, T. Michels-Clark, I. D Young, N. K Sauter, G. Evans, *Acta Cryst. D*, 2018, **74**, 85-97.

[7] P. R. Evans, G. N. Murshudov, *Acta Cryst. D*, 2013, **69**, 1204-1214.

[8] G. M. Sheldrick, *Acta Cryst. A* 2015, **71**, 3-8.

[9] G. M. Sheldrick, *Acta Cryst. C* 2015, **71**, 3-8.

[10] A. L. Spek, *Acta Cryst. C* 2015, **71**, 9-18.

for the final refinement as a 2-component twin. In the structures of **1**, **1a**, **2**, **2a** and **3**, a portion of the lattice solvent molecules were too diffuse/disordered to be modelled satisfactorily. The corresponding void spaces were thus analysed and taken into account with PLATON/SQUEEZE,[10] the formula reflecting the squeezed content. Poor diffraction results in a resolution lower than the IUCr recommendations in the case of compound 3.

All details can be found in CCDC 2172376-2172377-2172378-2172379-2172380-2172381 (**1**-**1a**-**2**-**2a**-**3**-**4**) which contain the supplementary crystallographic data for this paper. These data can be obtained free of charge from The Cambridge Crystallographic Data Center via https://summary.ccdc.cam.ac.uk/structure-summary-form. Crystallographic and refinement parameters are summarized in Table S1**,** while Tables S2 and S3 provide Fe–N bond lengths and details of hydrogen bonds involving the guest anion in the structures of **1**,**1a**, **2**, **2a**, **3** and **4**.

Table S1. Crystallographic and refinement parameters for the structure of compounds $SiF_6@[Fe_2(L1)(L2)_2](PF_6)_2\cdot ether\cdot MeOH$ (**1**), $SiF_6@[Fe_2(L1)(L3)_2](BF_4)_2\cdot MeOH$ (**1a**), $SiF_6@[Fe_2(L1)(L2)_2](PF_6)_2\cdot 2MeOH\cdot toluene$ (**2**), $SiF_6@[Fe_2(L1)(L3)_2](BF_4)_2\cdot MeOH\cdot 4dmf$ (**2a**), $ClO_4@[Fe_2(L2)_3](ClO_4)_3\cdot 20MeCN$ (**3**) and $ClO_4@[Fe_2(L3)_3](ClO_4)_3\cdot 9.67MeOH\cdot 2H_2O$ (**4**).

Compound	**1**	**1a**	**2**	**2a**	**3**	**4**
Formula	$C_{83}H_{70}F_{18}Fe_2N_{18}O_2P_2Si$	$C_{79}H_{60}B_2F_{14}Fe_2N_{18}OSi$	$C_{91}H_{80}F_{18}Fe_2N_{18}O_2P_2Si$	$C_{95}H_{96}B_2F_{14}Fe_2N_{22}O_5Si$	$C_{124}H_{120}Cl_4Fe_2N_{38}O_{16}$	$C_{99.67}H_{114.67}Cl_4Fe_2N_{18}O_{27.67}$
FW (g mol^{-1})	1895.29	1704.85	2001.46	2053.34	2652.05	2260.95
Wavelength (Å)	0.7288	0.72932	0.72932	0.72932	0.71073	0.72932
T (K)	100(2)	100(2)	100(2)	100(2)	100(2)	100(2)
Crystal system	monoclinic	monoclinic	monoclinic	tetragonal	triclinic	monoclinic
Space group	$P2_1/c$	$P2_1/c$	Cc	$P4_12_12$	$P-1$	$P2_1/n$
a (Å)	17.2482(8)	17.310(3)	22.696(4)	30.215(4)	18.685(2)	23.217(5)
b (Å)	26.1224(12)	25.070(5)	27.095(5)	30.215(4)	19.364(2)	17.634(3)
c (Å)	18.8989(9)	18.781(4)	17.870(4)	21.126(4)	19.401(2)	27.292(5)
α (°)	90	90	90	90	68.021(6)	90
β (°)	105.110(2)	105.202(5)	125.911(10)	90	88.515(7)	95.498(3)
γ (°)	90	90	90	90	67.719(6)	90
V (Å^3)	8220.8(7)	7865(3)	8900(3)	19287(6)	5968.1(11)	11122(4)
Z	4	4	4	8	2	4
ρ_{calcd} (g cm^{-3})	1.531	1.440	1.494	1.415	1.475	1.350
μ (mm^{-1})	0.547	0.514	0.524	0.461	0.524	0.473
Reflections	15186	12463	20656	15347	7187	27023
R_{int}	0.0255	0.0195	0.0813	0.0215	0.0735	0.0433
Restraints	422	257	306	377	1776	418
Parameters	1202	1073	1212	1165	1276	1436
S	1.064	1.019	1.061	1.038	1.069	1.043
R_1 [$I>2\sigma(I)$]	0.0682	0.1137	0.0526	0.0799	0.0999	0.1285
wR_2 [$I>2\sigma(I)$]	0.2064	0.2796	0.1483	0.2312	0.2821	0.4025
R_1 [all data]	0.0791	0.1307	0.0536	0.0838	0.1385	0.1389
wR_2 [all data]	0.2190	0.2921	0.1496	0.2422	0.3245	0.4114
Largest peak / hole (e Å^3)	1.479 / –1.383	3.217 / –0.745	1.339 / –0.772	0.580 / –0.502	0.854 / –0.695	1.560 / –0.945

Table S2. Fe-N bond lengths in the structures of compounds **1**, **1a**, **2**, **2a**, **3** and **4**.

	1	**1a**	**2**	**2a**	**3**	**4**
Fe1–N1	2.230(3)	2.224(7)	2.225(4)	2.241(7)	2.009(12)	1.993(5)
Fe1–N2	2.156(4)	2.143(8)	2.175(3)	2.155(7)	1.950(13)	1.964(5)
Fe1–N7	2.162(3)	2.180(7)	2.218(3)	2.240(9)	1.964(12)	1.999(5)
Fe1–N8	2.166(3)	2.133(7)	2.155(3)	2.176(7)	1.967(12)	1.961(5)
Fe1–N13	2.219(4)	2.203(8)	2.206(3)	2.258(6)	1.994(12)	2.022(5)
Fe1–N14	2.118(3)	2.151(7)	2.153(3)	2.153(6)	1.971(13)	1.979(5)
Fe2–N5	2.115(4)	2.023(6)	1.999(4)	2.181(6)	1.918(12)	1.941(6)
Fe2–N6	2.149(5)	2.048(6)	2.048(4)	2.194(6)	2.002(12)	1.997(6)
Fe2–N11	2.103(3)	1.988(9)	2.025(3)	2.119(7)	1.964(12)	1.949(6)
Fe2–N12	2.176(4)	2.104(7)	2.060(3)	2.203(8)	2.003(12)	1.989(6)
Fe2–N17	2.095(4)	2.002(6)	2.010(4)	2.104(7)	1.952(13)	1.941(6)
Fe2–N18	2.182(3)	2.071(7)	2.039(4)	2.273(6)	1.986(12)	1.993(6)
<Fe1–N>	2.17(2)	2.17(4)	2.19(2)	2.20(4)	1.98(7)	1.99(3)
<Fe2–N>	2.14(2)	2.04(3)	2.03(2)	2.18(4)	1.97(7)	1.97(4)

Table S3. Hydrogen bonds involving the guest anion in the structures of compounds **1**, **1a**, **2**, **2a**, **3** and **4**.

	D–H···A	D–H (Å)	H···A (Å)	D···A (Å)	D–H···A (º)
1	N3–H3···F3	0.83(5)	2.00(5)	2.782(4)	158(5)
	N4–H4···F6	0.93(6)	1.81(6)	2.721(4)	167(5)
	N9–H9···F1	0.81(5)	1.93(5)	2.736(4)	169(5)
	N10–H10···F5	0.87(6)	2.27(6)	3.065(4)	152(6)
	N15–H15···F2	0.89(5)	1.82(5)	2.713(4)	175(5)
	N16–H16···F4	0.82(6)	1.82(6)	2.626(4)	171(6)
1a	N3–H3B···F4	0.88	2.44	3.144(7)	137.3
	N4–H4B···F1	0.88	1.92	2.736(7)	152.6
	N9–H9A···F5	0.88	1.84	2.720(7)	173.1
	N10–H10B···F2	0.88	2.00	2.787(7)	147.6
	N15–H15A···F6	0.88	1.81	2.621(8)	152.5
	N16–H16B···F3	0.88	1.90	2.722(8)	155.0
2	N3–H3B···F2	0.88	2.03	2.876(4)	161.3
	N4–H4A···F5	0.88	1.94	2.746(4)	152.2
	N9–H9A···F6	0.88	1.90	2.726(4)	155.8
	N10–H10A···F3	0.88	2.20	2.960(4)	144.9
	N15–H15B···F1	0.88	1.82	2.665(4)	159.4
	N16–H16A···F4	0.88	1.84	2.632(4)	149.0
2a	N3–H3A···F5	0.88	1.86	2.730(7)	169.0
	N4–H4B···F2	0.88	2.13	2.986(9)	164.7
	N9–H9A···F6	0.88	2.05	2.916(10)	169.3
	N10–H10B···F3	0.88	1.87	2.743(10)	170.1
	N15–H15A···F1	0.88	1.83	2.667(8)	159.2
	N16–H16B···F4	0.88	1.90	2.709(6)	152.8
3	N3–H3B···N2S	0.88	2.11	2.99(2)	175.7
	N10–H10B···O2	0.88	2.44	3.094(17)	131.2
	N16–H16B···O3	0.88	2.13	2.923(18)	149.3
4	N3–H3A···O1	0.88	2.23	3.019(7)	148.8
	N4–H4B···O4S	0.88	1.92	2.755(7)	158.5
	N9–H9A···O4	0.88	2.39	3.102(11)	138.5
	N9–H9A···O2S	0.88	1.99	2.733(9)	141.1
	N10–H10B···O1W	0.88	1.98	2.859(7)	176.7
	N15–H15A···O1S	0.88	1.88	2.745(9)	167.0
	N16–H16B···O3S	0.88	1.91	2.774(10)	168.4
	O1S–H1S···O2	0.92(2)	2.06(4)	2.904(13)	153(8)
	O3S–H3S···O3	1.07	2.08	2.987(12)	141.1
	O1W–H1W···O2	0.92(2)	1.98(4)	2.860(9)	161(9)

Magnetometry

Variable-temperature magnetic measurements were performed using a Quantum Design MPMS-XL SQUID magnetometer at the "Unitat de Mesures Magnètiques" of the Universitat de Barcelona. The diamagnetic contributions to the susceptibility were corrected using Pascal's constant tables. Further corrections of the sample holders contribution, determined empirically, were also applied. Variable temperature *dc* data were collected with an applied field of 5000 Oe, in settle mode.

Other Physical Measurements

Elemental analyses were performed with a Perkin-Elmer Series II CHNS/O Analyzer 2400 (C, H, N) at the Servei de Microanàlisi of CSIC, Barcelona. IR spectra were recorded as KBr pellet samples on a Nicolet 5700 FTIR spectrometer. ^{1}HNMR and ^{19}F NMR were performed, respectively, in acetone and acetonitrile, on a Bruker 400 MHz Avance III and a Bruker Avance Neo de 500 MHz apparatus at room temperature. The sample for ^{19}F NMR was prepared by dissolving compound **2a** in CD_3CN under stirring for 20 min within a plastic container and transferred to an NMR quartz tube after filtration with Celite. After determination of the spectrum, a solution (0.2mL) of $(Bu_4N)_2SiF_6$ (3 mg) in CD_3CN (1 mL) was added to the tube, before acquisition of the second spectrum.

DFT Calculations

The reaction energy of the process $(PF_6@[Fe_2(L1)(L')_2])^{3+} + SiF_6^{2-} \rightarrow (SiF_6@[Fe_2(L1)(L')_2])^{2+} + PF_6^-$ (L' = L2 and L3) was evaluated after fully optimizing the geometry of each species. These structural optimizations were carried out using density functional theory (DFT) based calculations employing the PBE[11] functional and an Ahlrichs TZVP basis set[12] using the Gaussian16 code.[13] The structure and energy in solution of each species was computed using the polarizable continuum model.[14] Spin-unrestricted calculations were done when dealing with the helicates because the high-spin of the Fe(II) ions were considered. In all the calculations, a semi-empirical dispersion potential introduced by Grimme was added to the conventional Kohn–Sham

---

[11] J.P. Perdew, K. Burke, M. Ernzerhof, *Phys. Rev. Lett*. 1996, **77**, 3865–3868.

[12] A. Schäfer, C. Huber, R. Ahlrichs, *J. Chem. Phys*. 1994, **100**, 5829–5835.

[13] Gaussian 16, Revision B.01, M. J. Frisch, G. W. Trucks, H. B. Schlegel, G. E. Scuseria, M. A. Robb, J. R. Cheeseman, G. Scalmani, V. Barone, G. A. Petersson, H. Nakatsuji, X. Li, M. Caricato, A. V. Marenich, J. Bloino, B. G. Janesko, R. Gomperts, B. Mennucci, H. P. Hratchian, J. V. Ortiz, A. F. Izmaylov, J. L. Sonnenberg, D. Williams-Young, F. Ding, F. Lipparini, F. Egidi, J. Goings, B. Peng, A. Petrone, T. Henderson, D. Ranasinghe, V. G. Zakrzewski, J. Gao, N. Rega, G. Zheng, W. Liang, M. Hada, M. Ehara, K. Toyota, R. Fukuda, J. Hasegawa, M. Ishida, T. Nakajima, Y. Honda, O. Kitao, H. Nakai, T. Vreven, K. Throssell, J. A. Montgomery, Jr., J. E. Peralta, F. Ogliaro, M. J. Bearpark, J. J. Heyd, E. N. Brothers, K. N. Kudin, V. N. Staroverov, T. A. Keith, R. Kobayashi, J. Normand, K. Raghavachari, A. P. Rendell, J. C. Burant, S. S. Iyengar, J. Tomasi, M. Cossi, J. M. Millam, M. Klene, C. Adamo, R. Cammi, J. W. Ochterski, R. L. Martin, K. Morokuma, O. Farkas, J. B. Foresman, and D. J. Fox, Gaussian, Inc., Wallingford CT, 2016.

[14] J. Tomasi, B. Mennucci, and R. Cammi, "Quantum mechanical continuum solvation models," *Chem. Rev.*, 2005, **105**, 2999-3093.

DFT energy in order to properly describe the van der Waals interactions. Specifically, the so-called DFT-D3(BJ) parametrization was used.[15]

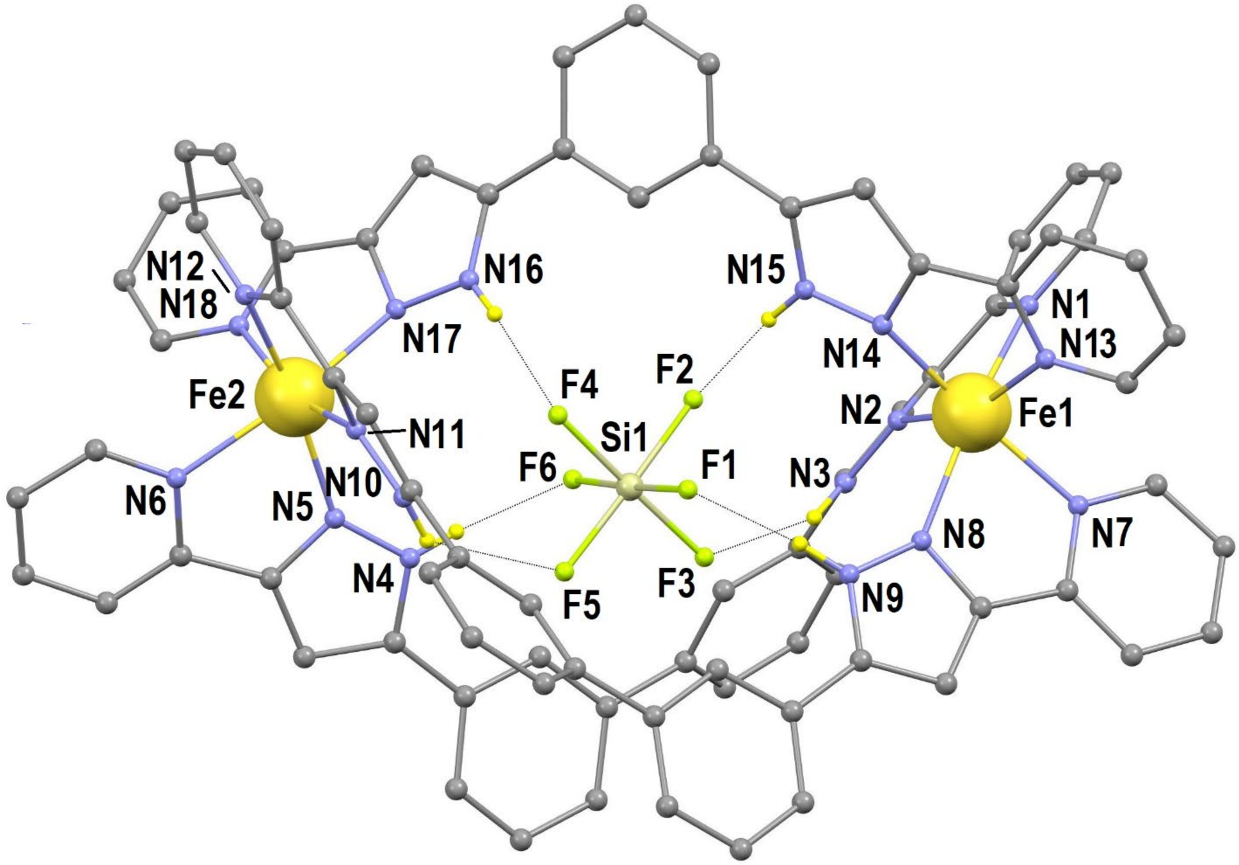

Figure S1. Representation of the supramolecular $(SiF_6@[Fe_2(L1)(L2)_2])^{2+}$ cationic moiety of **1**, with heteroatoms labelled, emphasizing the H-bonding interactions (black dashed lines, see Table S3 for details) between the central SiF_6^{2-} guest and the $[Fe_2(L1)(L2)_2]^{4+}$ host. Grey atoms are C. Only H atoms (yellow) from N−H groups shown.

---

[15] S. Grimme, S. Ehrlich and L. Goerigk, *J. Comp. Chem*. 2011, **32**, 1456-65.

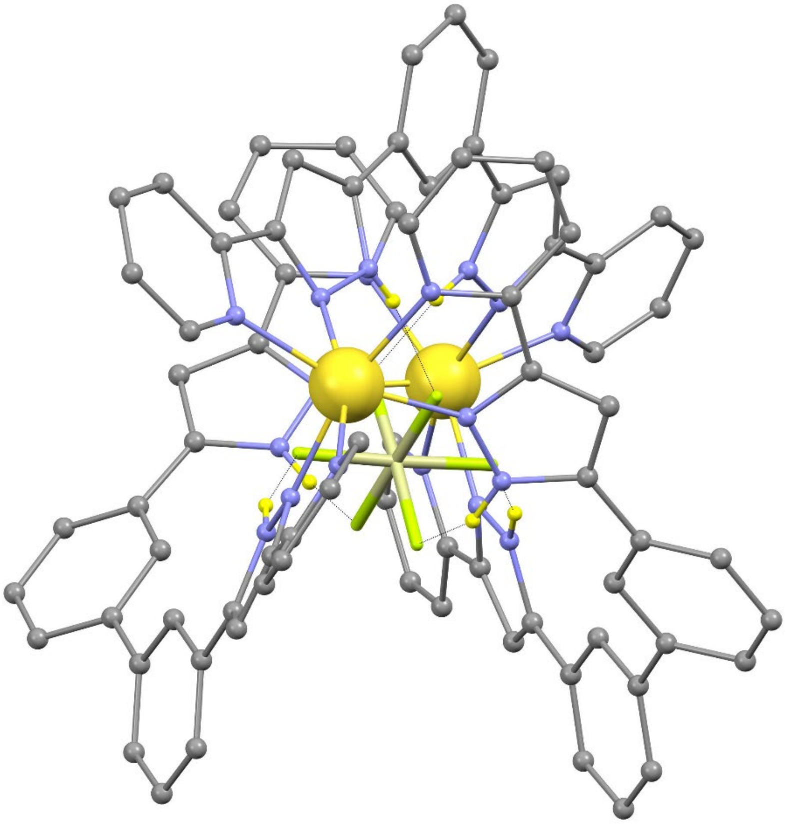

Figure S2. Perspective view of the (SiF_6@[Fe_2(L1)(L2)$_2$])$^{2+}$ assembly in **1**, approximately down the Fe···Fe axis, emphasizing that the mass center of the SiF_6^{2-} guest is significantly removed from this axis due to the asymmetry caused by the length difference between ligands L1 and L2. Colour code as in Fig S1. Hydrogen bonds are black dashed lines

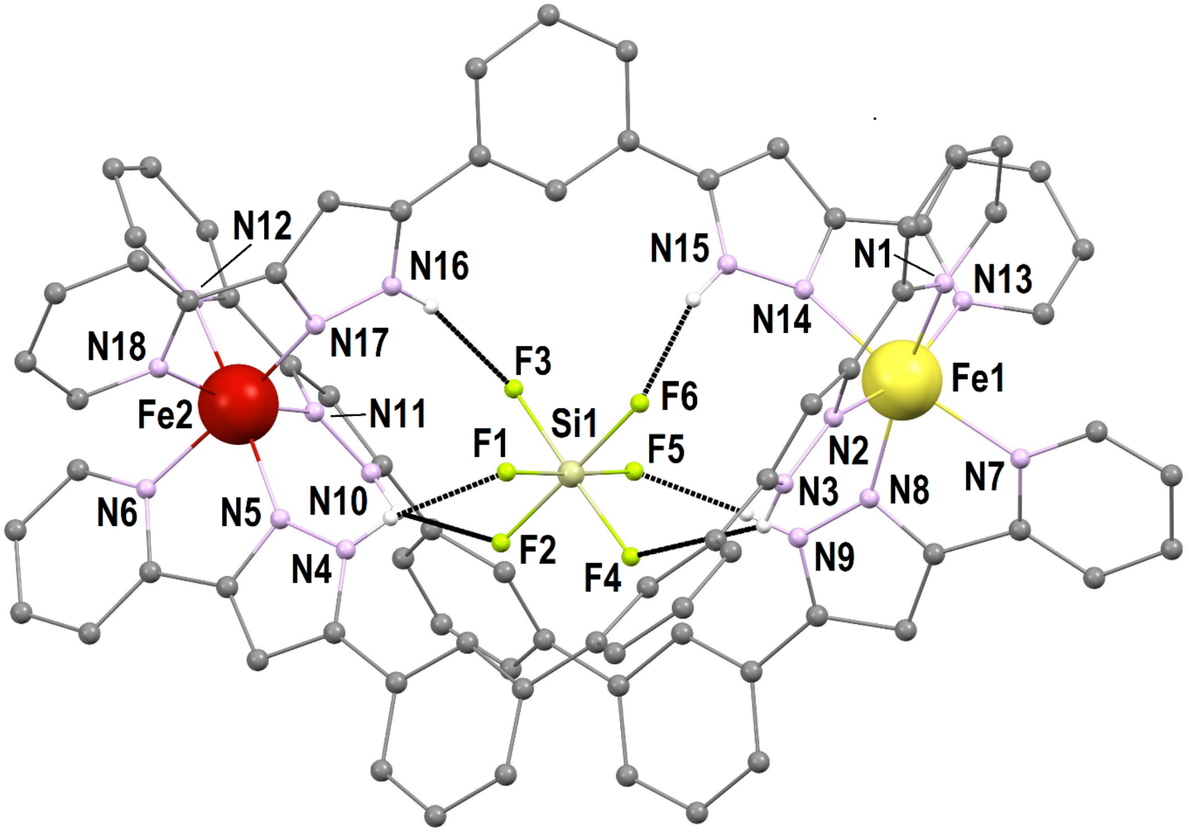

Figure S3. Representation of the supramolecular $(SiF_6@[Fe_2(L1)(L2)_2])^{2+}$ cationic moiety of **1a**, with heteroatoms labelled, emphasizing the H-bonding interactions (black dashed lines, see Table S3 for details) between the central SiF_6^{2-} guest and the $[Fe_2(L1)(L2)_2]^{4+}$ host. Grey atoms are C. Only H atoms (white) from N−H groups shown.

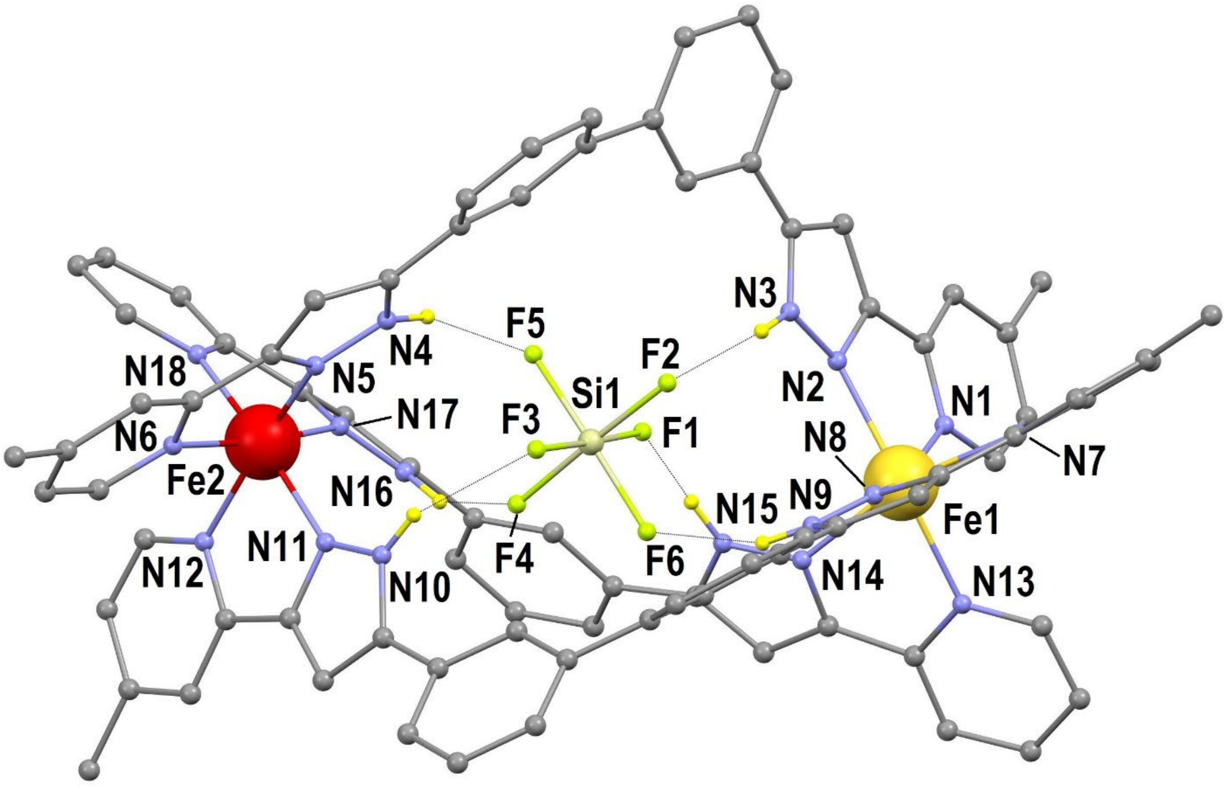

Figure S4. Representation of the supramolecular $(SiF_6@[Fe_2(L1)(L3)_2])^{2+}$ cationic moiety of **2**, with heteroatoms labelled, emphasizing the H-bonding interactions (black dashed lines, see Table S3 for details) between the central SiF_6^{2-} guest and the $[Fe_2(L1)(L3)_2]^{4+}$ host. Grey atoms are C. Only H atoms (yellow) from N−H groups shown.

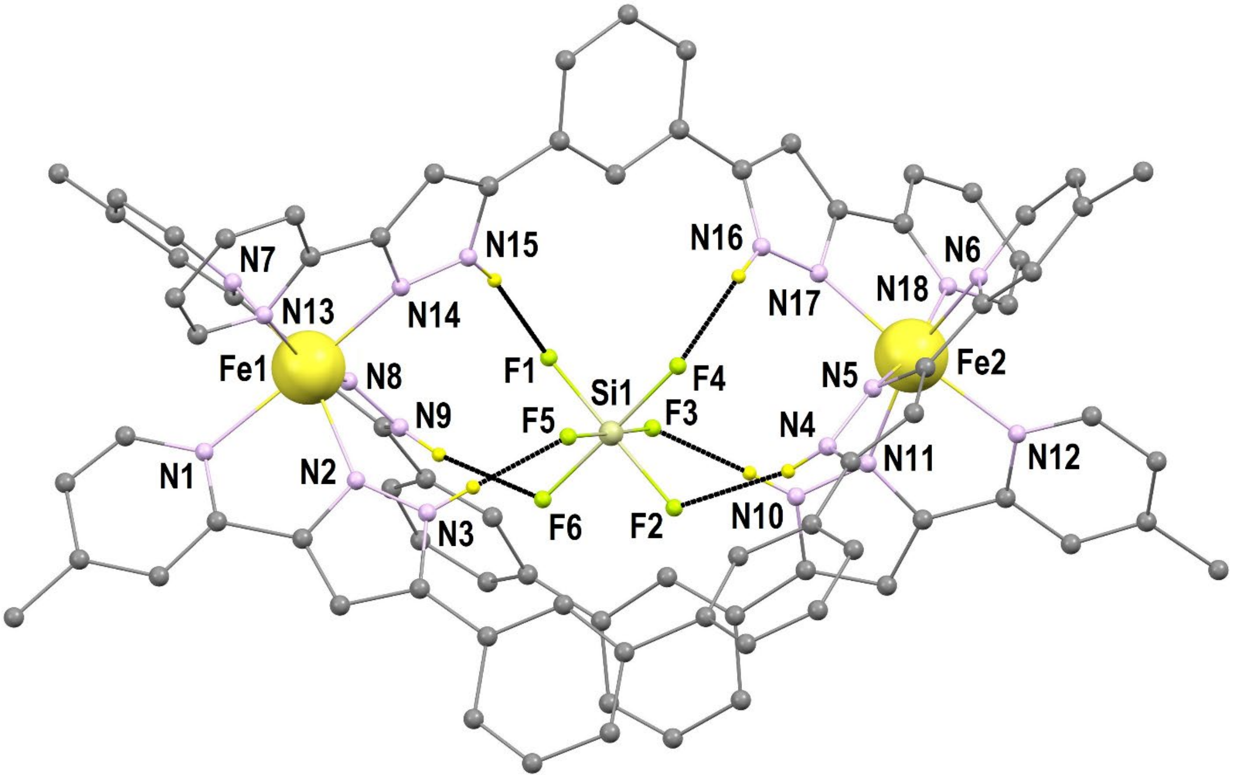

Figure S5. Representation of the supramolecular $(SiF_6@[Fe_2(L1)(L3)_2])^{2+}$ cationic moiety of **2a**, with heteroatoms labelled, emphasizing the H-bonding interactions (black dashed lines, see Table S3 for details) between the central SiF_6^{2-} guest and the $[Fe_2(L1)(L3)_2]^{4+}$ host. Grey atoms are C. Only H atoms (yellow) from N−H groups shown.

1

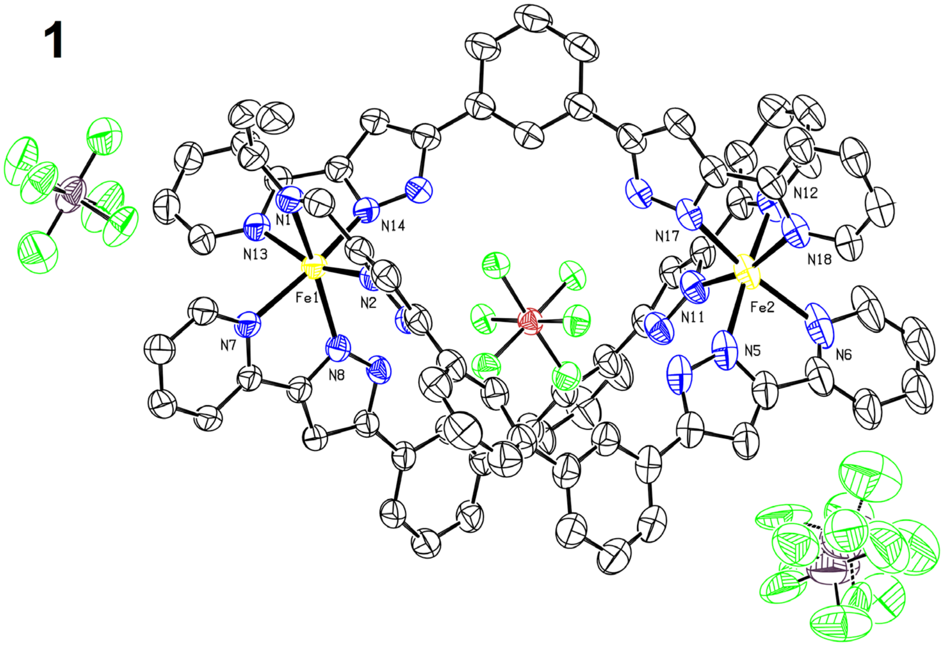

1a

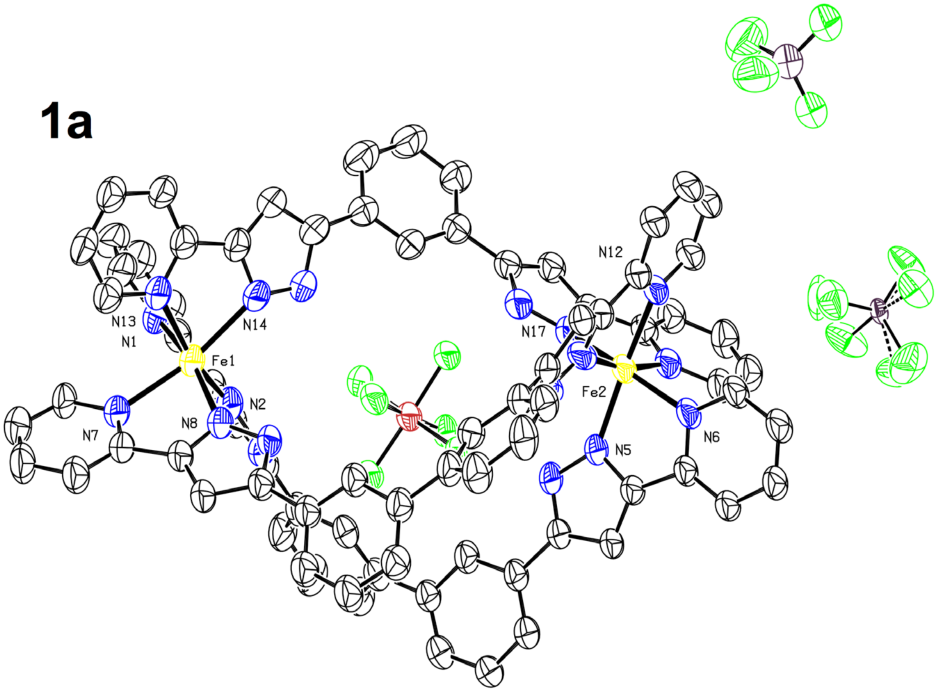

Figure S6. ORTEP views of the structures of compounds **1** (top, 50 % probability) and **1a** (bottom, 30 % probability).

2

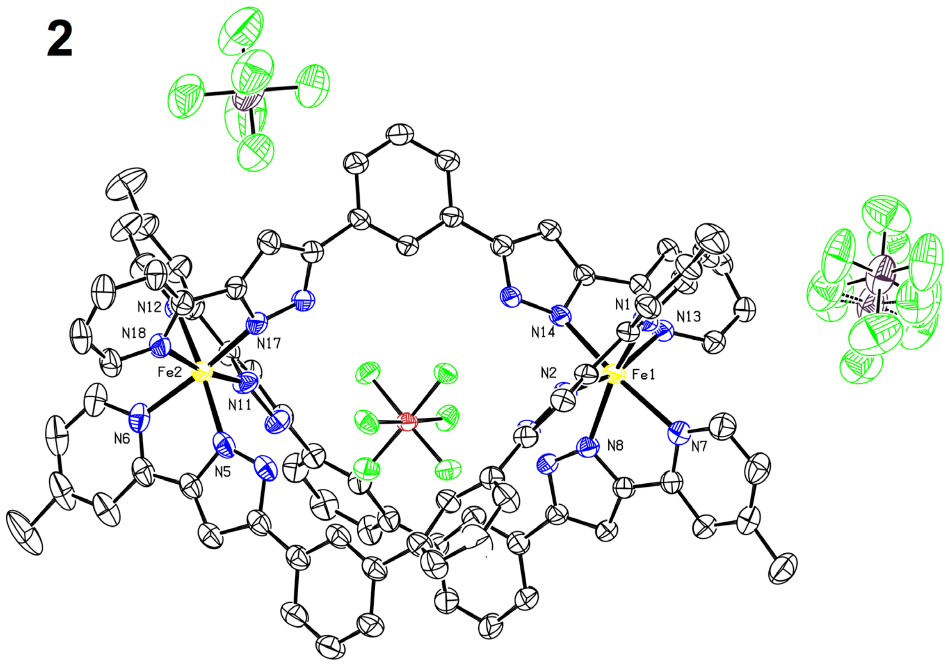

2a

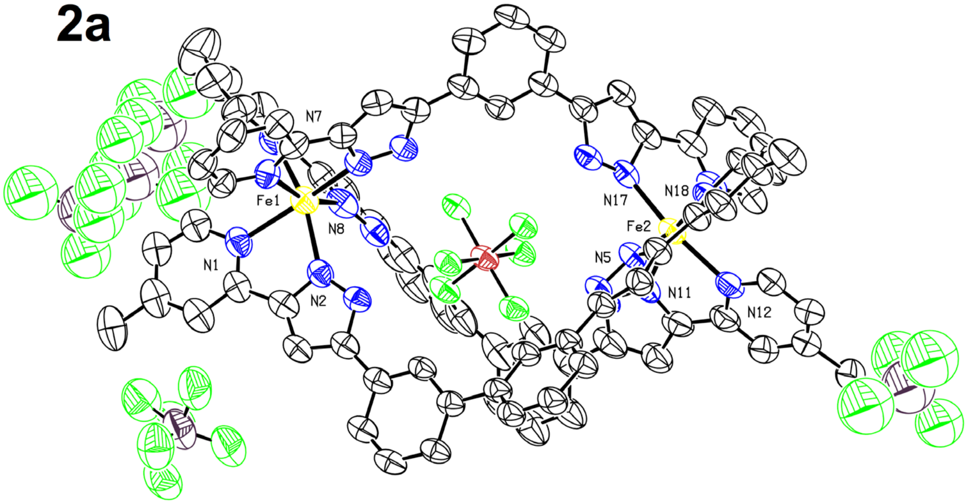

Figure S7. ORTEP views of the structures of compounds **2** (top, 50 % probability) and **2a** (bottom, 30 % probability).

3

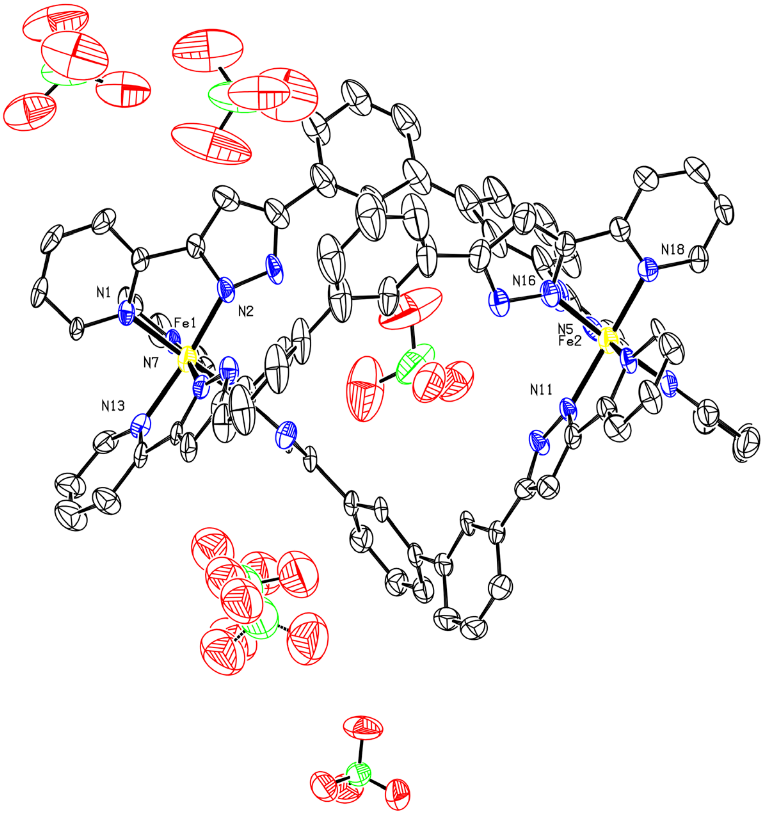

4

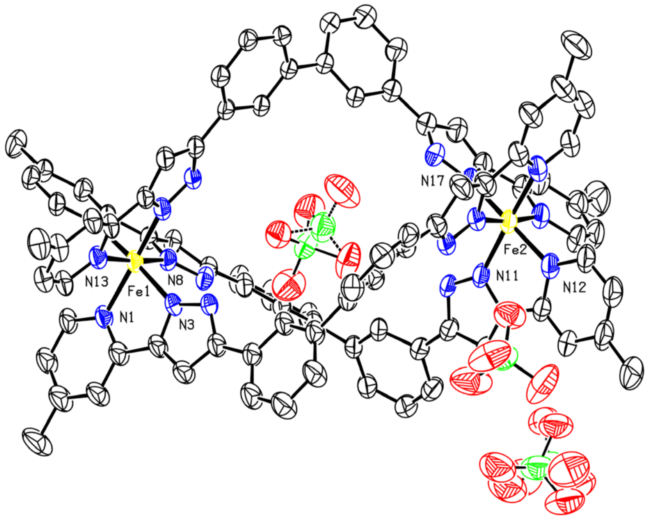

Figure S8. ORTEP views of the structures of compounds **3** (top, 50 % probability) and **4** (bottom, 50 % probability).

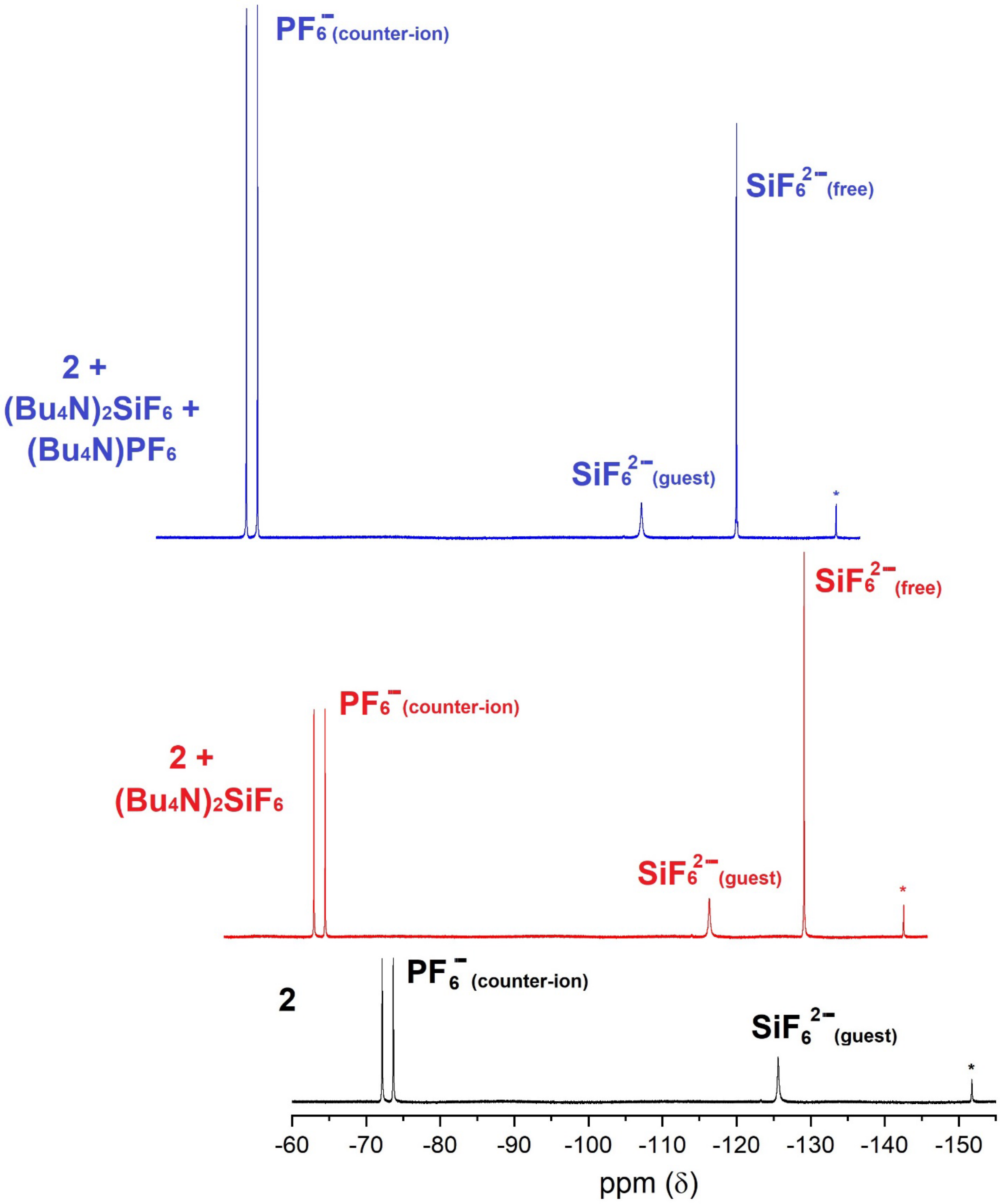

Figure S9. ^{19}F NMR spectra in MeCN of SiF_6@[Fe(L1)(L3)$_2$](PF_6)$_2$ (**2**, black trace), and of **2** + ~2 eq of $(Bu_4N)_2SiF_6$ (red trace, shifted wrt to the bottom scale) and after subsequent addition of excess $(Bu_4N)PF_6$ (blue trace, further shifted). The small peak marked with '*' is an impurity coming from the glass, often detected in similar experiments with other systems.

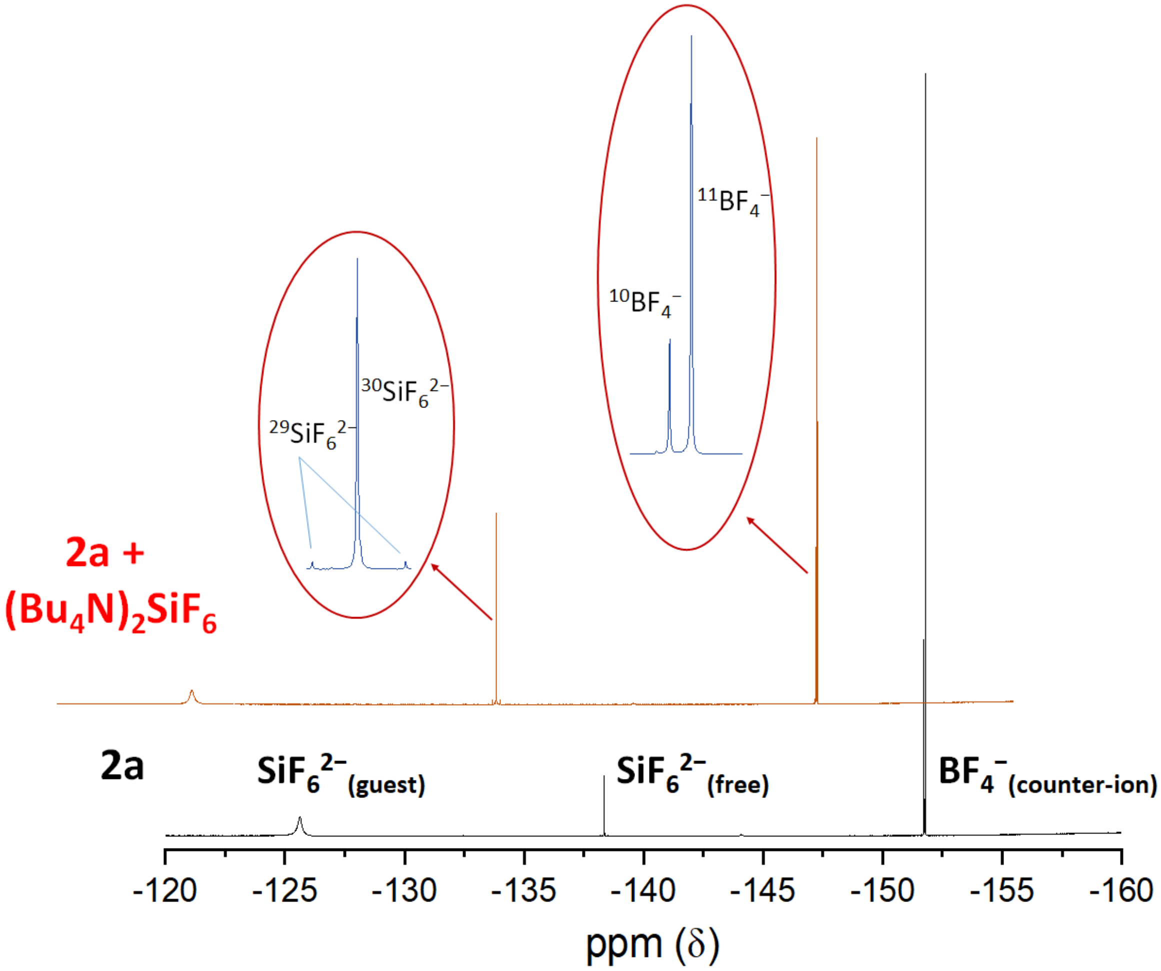

Figure S10. ^{19}F NMR spectra in MeCN of SiF_6@[Fe(L1)(L3)$_2$](BF_4)$_2$ (**2a**, black trace) and of **2a** + ~1 eq of $(Bu_4N)_2SiF_6$ (red trace, shifted wrt to the bottom scale). The peaks from free SiF_6^{2-} and free BF_4^{4-} have been expanded, emphasizing the satellites from coupling with ^{29}Si (I = 1/2, 4.7% abundance) and the different ^{19}F chemical shift for $^{11}BF_4^-$ (~80%) and $^{10}BF_4^-$ (~20%), respectively.

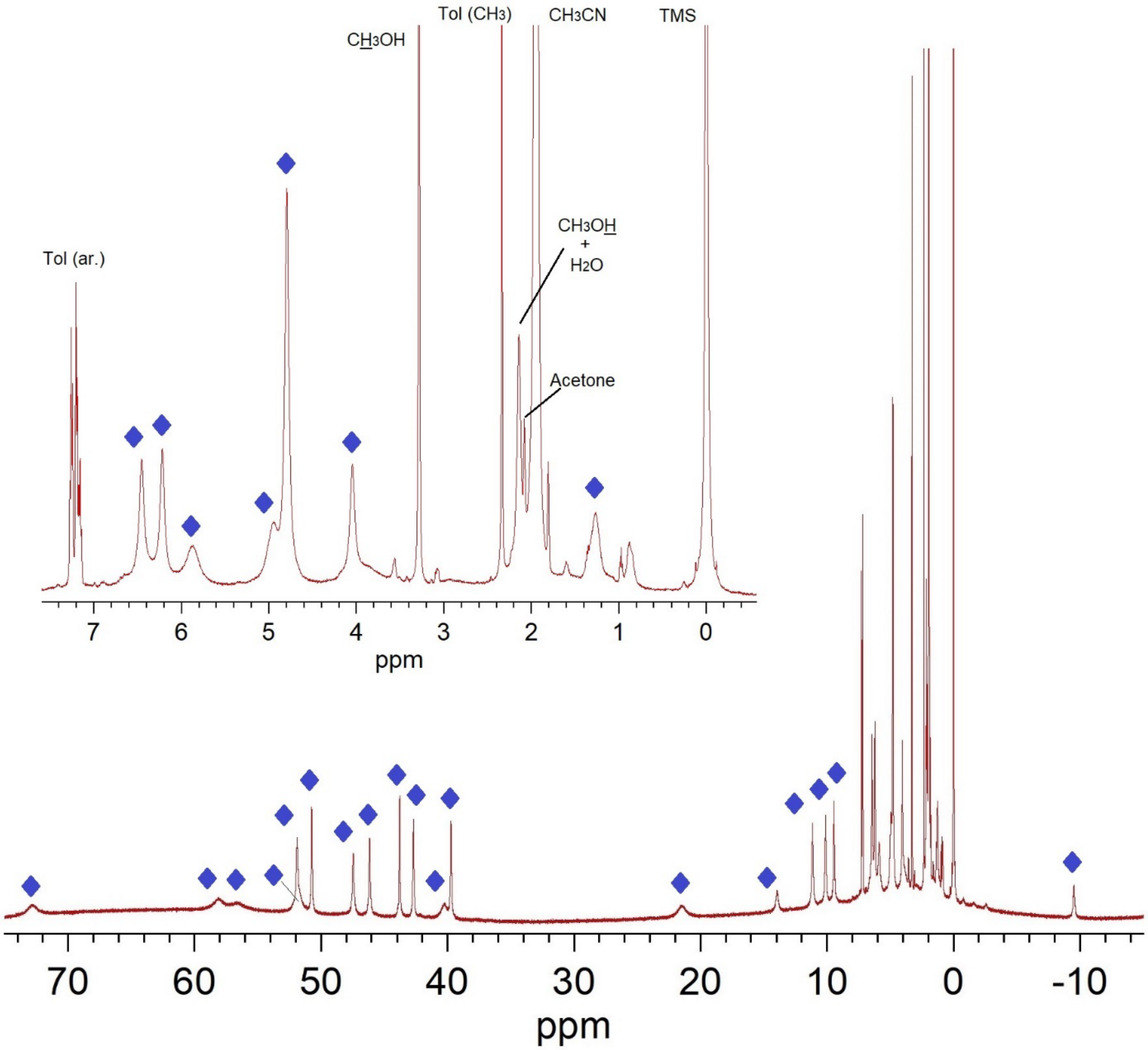

Figure S11. ^{1}H NMR spectrum in MeCN of SiF_6@[Fe(L1)(L3)$_2$](PF_6)$_2$ (**2a**, the inset shows the diamagnetic region). Blue rhombuses mark the 25 broadened and paramagnetically shifted peaks expected from the idealized C_2 symmetry of SiF_6@[Fe(L1)(L3)$_2$]$^{2+}$, if both rings of the biphenyl in L3 are made equivalent by virtue of the fluxionality around the single C−C bonds holding them. The remaining relevant peaks are diamagnetic and have been identified as the solvents used. The ^{1}H NMR spectra after adding (Bu_4N)$_2SiF_6$ and (Bu_4N)PF_6 are identical (except for the additional peaks from the organic cation).

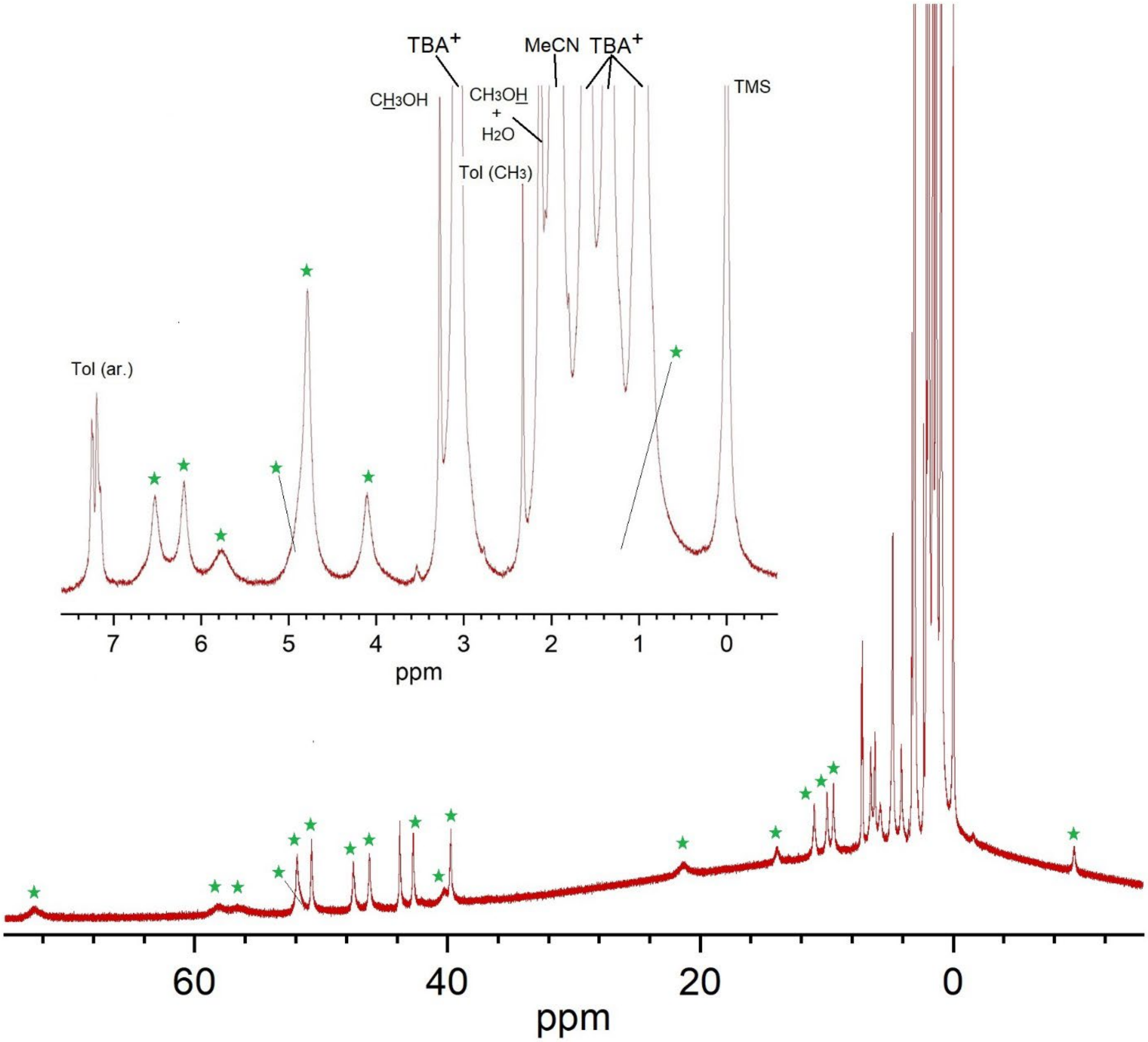

Figure S12. ^{1}H NMR spectrum in MeCN of SiF_6@[Fe(L1)(L3)$_2$]$(PF_6)_2$ (**2a**) after addition of solid $(Bu_4N)_2SiF_6$ (~2 eq) and $(Bu_4N)PF_6$ (excess). The peaks from the SiF_6@[Fe(L1)(L3)$_2$]$^{2+}$ species are preserved, confirming the invariable presence of one sole compound.

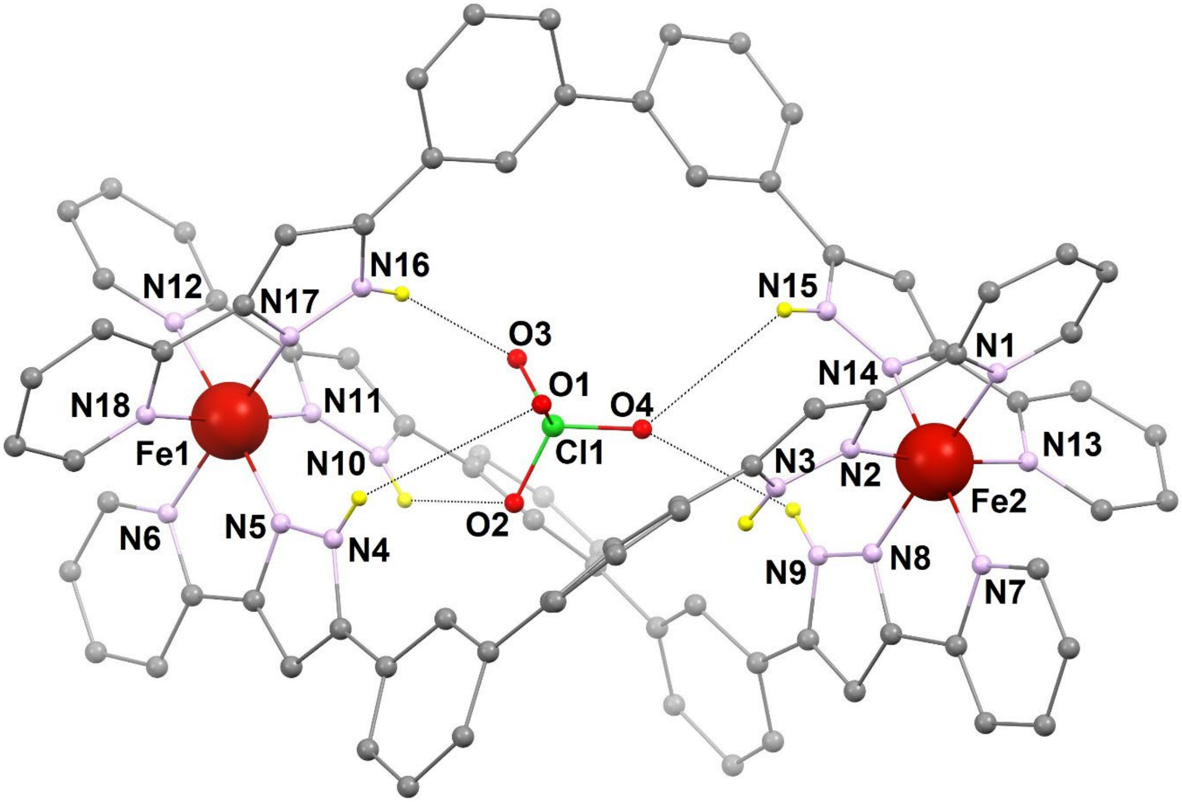

Figure S13. Representation of the supramolecular $(ClO_4@[Fe_2(L2)_3])^{3+}$ cationic moiety of **3**, with heteroatoms labelled, emphasizing the H-bonding interactions (black dashed lines, see Table S3 for details) between the central ClO_4^- guest and the $[Fe_2(L2)_3]^{4+}$ host. Grey atoms are C. Only H atoms (yellow) from N−H groups shown.

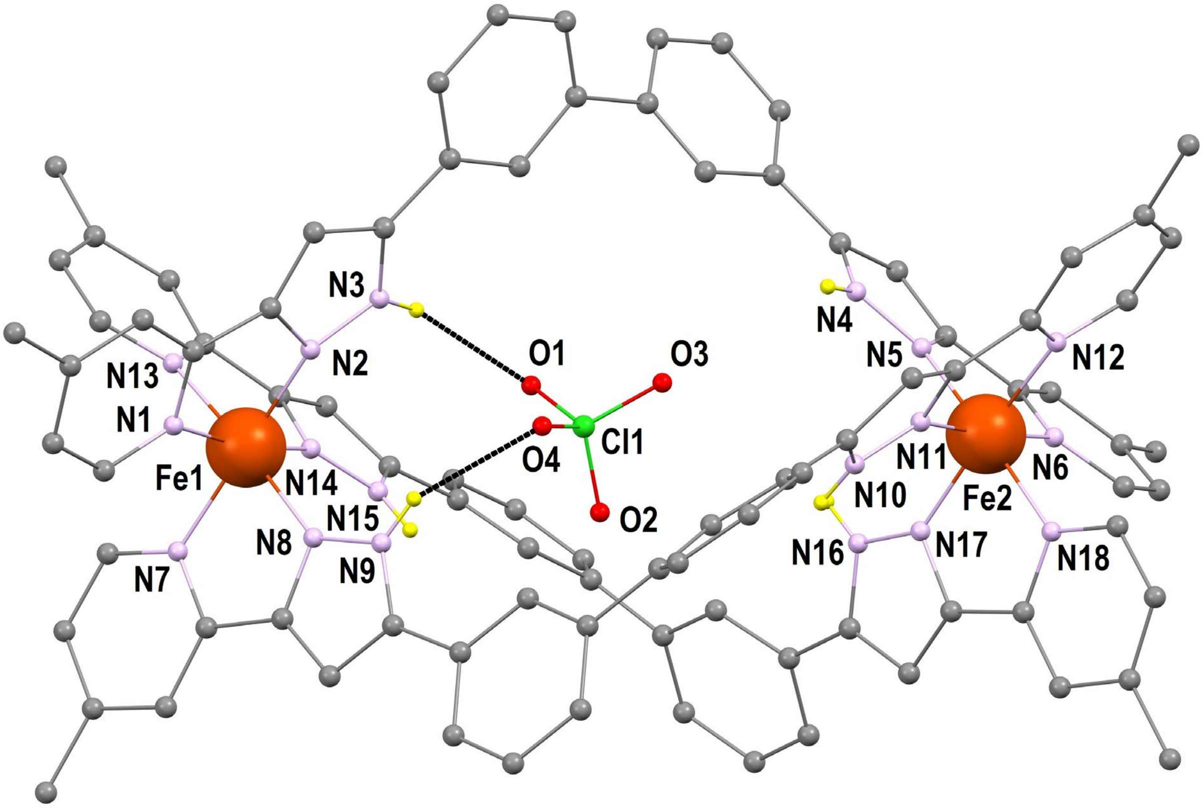

Figure S14. Representation of the supramolecular $(ClO_4@[Fe_2(L3)_3])^{3+}$ cationic moiety of **4**, with heteroatoms labelled, emphasizing the H-bonding interactions (black dashed lines, see Table S3 for details) between the central ClO_4^- guest and the $[Fe_2(L3)_3]^{4+}$ host. Grey atoms are C. Only H atoms (yellow) from N−H groups shown.